Matrix Isolation and ab Initio Study of 1:1 Hydrogen-Bonded Complexes of H_2O_2 with HF, HCl, and HBr

James R. Goebel, Kathryn A. Antle, and Bruce S. Ault*

Department of Chemistry, University of Cincinnati, P.O. Box 210172, Cincinnati, Ohio 45221-0172

Janet E. Del Bene

Department of Chemistry, Youngstown State University, Youngstown, Ohio 44555, and Quantum Theory Project, University of Florida, Gainesville, Florida 32611

Received: February 26, 2002; In Final Form: May 2, 2002

Matrix isolation infrared spectroscopy has been combined with MP2/aug′-cc-pVDZ calculations to characterize the 1:1 hydrogen-bonded complexes between H_2O_2 and the hydrogen halides HF, HCl, and HBr. The infrared spectra of the these complexes are characterized by an intense, red-shifted H−X stretching band, as well as slight perturbations to several of the HOOH vibrational bands. For the HF complex, the intermolecular librational modes were also observed. The ab initio calculations identified two equilibrium structures on each surface, one an open structure, and the other cyclic. These two structures have similar binding energies. However, only the open structure appears to be present in argon and nitrogen matrices. This open structure is preferentially stabilized by interaction of its larger dipole moment with the matrix medium.

Introduction

Hydrogen peroxide is a molecule that is of interest in a large and diverse number of fields, including atmospheric chemistry and biochemistry.[1−3] Until recently, gas phase, solvent-free studies of H_2O_2 were technically difficult. However, the development[4] and use of the hydrogen peroxide−urea complex (UHP) as a safe source of solvent-free gas-phase H_2O_2 has allowed initial studies[5,6] of the hydrogen-bonding capability of H_2O_2. This is an important development, since solution studies are complicated by the role of the solvent, to the extent that hydrogen peroxide had not been well characterized previously in hydrogen-bonded complexes. Using this technology, combined with matrix isolation spectroscopy[7−9] and high level ab initio calculations, a recent series of papers[10−12] have examined hydrogen-bonded complexes with H_2O_2 as a proton donor to a range of lone pair electron donors, including nitrogen, oxygen, phosphorus, and sulfur bases.

The role of H_2O_2 as a proton acceptor in a hydrogen bond has not been well characterized. The recent report[6] of a cyclic complex between H_2O_2 and H_2O provides the only example to date of an isolated complex in which H_2O_2 accepts a proton from a donor molecule in a hydrogen-bonded species. However, this study was complicated by very low product band intensities and the cyclic nature of the reported complex. To further explore the ability of H_2O_2 to participate in hydrogen bonds, a joint experimental and theoretical study was undertaken to characterize the hydrogen-bonded complexes of H_2O_2 with the hydrogen halides HF, HCl, and HBr. These hydrogen halides are well-known as proton donors[13−16] in a wide range of hydrogen-bonded complexes. The present study provides the first evidence of hydrogen-bonded complexes in which H_2O_2 serves solely as a proton acceptor. In this paper, the structural, energetic, and spectral properties of these complexes will be presented and discussed.

* Author to whom correspondence should be addressed.

Experimental Section

All of the experiments in this study were carried out on conventional matrix isolation equipment,[17] with modification for the generation and deposition of H_2O_2, as described previously.[11] In these experiments, the matrix gas was swept over a sample of the solid H_2O_2:urea adduct (UHP, Aldrich), or its perdeuterated counterpart (produced by the repeated exchange of the UHP adduct with D_2O, followed by vacuum-drying). The H_2O_2 vapor in equilibrium with the adduct was carried with the matrix gas to the cold window and deposited. The temperature range for the vaporization of H_2O_2 in these experiments was 9−18 °C, which provided the means to control the sample concentration. HF, HCl, and HBr (all Matheson) and DCl (Cambridge Isotope Laboratories) were introduced into the vacuum system from lecture bottles, and purified by repeated freeze−pump−thaw cycles at 77 K. HF adsorbed very strongly to the stainless steel manifold, so that accurate determination of the concentration of the Ar/HF samples could not be made. However, comparison to literature spectra provided a good estimate of the concentration. Argon and nitrogen (Wright Brothers) were used without further purification as the matrix gases in these experiments.

All of the experiments were conducted in the twin jet mode, in which samples of H_2O_2 (or D_2O_2) and the hydrogen halide were each diluted in the matrix gas and deposited from separate deposition lines onto the 14 K cold window. Experiments were conducted using a deposition rate between 4 and 15 mmol/h from each manifold for 3 h. Spectra were then recorded on a Mattson Cygnus FTIR at 1 cm^{-1} resolution. Many of the matrices were subsequently annealed to between 25 and 36 K and after re-cooling, additional spectra were recorded.

Method of Calculation

Searches of the HF:H_2O_2, HCl:H_2O_2, and HBr:H_2O_2 potential surfaces resulted in the identification of two equilibrium

10.1021/jp020520b CCC: $22.00
Published on Web 06/01/2002

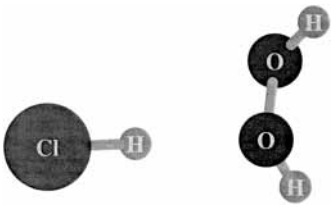

Figure 1. The structure of an open complex, illustrated by $ClH:O_2H_2$.

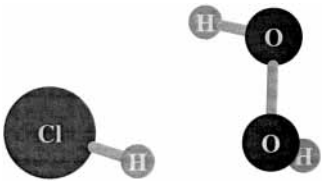

Figure 2. The structure of a cyclic complex, illustrated by HOOH:ClH.

structures on each surface, one an open structure, and the other cyclic. These will be differentiated as $XH:O_2H_2$ for the open structure which has the hydrogen halide as the proton donor to peroxide, and HOOH:XH for the cyclic structure in which both peroxide and the hydrogen halide are proton donors and proton acceptors. These structures are illustrated for $HCl:H_2O_2$ in Figures 1 and 2. The open and the cyclic structures, as well as the monomers HOOH, HF, HCl, and HBr, were fully optimized at second-order Møller-Plesset perturbation theory (MP2)[18−21] with the aug′-cc-pVDZ basis set, where aug′-cc-pVDZ is the Dunning aug-cc-pVDZ basis set[22−24] without diffuse functions on hydrogens. Harmonic vibrational frequencies were computed to establish that the optimized structures are equilibrium structures with no imaginary frequencies, to evaluate zero-point vibrational energies, and to simulate the vibrational spectra of the monomers and complexes. The aug′-cc-pVDZ basis set was used in this study since previous work[25] had demonstrated that this basis set seems to provide a better description of HCl than the 6-31+G(d,p) basis set.[26−29] The level of theory employed is capable of providing frequency shifts of the hydrogen-bonded X−H stretching band in agreement with experimental shifts, provided that anharmonicity corrections in the complexes are not unusually large. The harmonic vibrational spectra of the deuterated analogues of monomers and complexes have also been computed.

Searches of the potential surfaces were made in an attempt to identify transition structures which connect the equilibrium open and cyclic structures. Along one path the interconversion of these two structures can be accomplished through rotation of one O−H bond of H_2O_2 about the O−O bond. The barrier to interconversion along this path is essentially the barrier to rotation in isolated H_2O_2 from its equilibrium C_2 structure in which the H−O−O−H dihedral angle is 112.4°, through a trans C_{2h} structure with a dihedral angle of 180°. The computed electronic energy barrier to this rotation is 1.1 kcal/mol. However, an examination of the two equilibrium structures suggests that there should be a lower-energy path connecting the two structures through a rotation of the entire H_2O_2 molecule about the O−O axis, coordinated with a rotation of HX which bends the X−H···O hydrogen bond from its linear orientation in the open structure to a bent orientation in the cyclic structure. However, because the potential surfaces in the hydrogen-bonding region appear to be relatively flat, a transition structure of this type was not found.

Single-point MP2/aug′-cc-pVTZ calculations were carried out on the optimized monomers and complexes to obtain improved binding energies. The valence triple-split aug′-cc-pVTZ basis set is the aug-cc-pVTZ basis[22−24] with diffuse functions on all atoms except hydrogen. This basis set gives binding energies which approach basis-set converged binding energies, without correcting for basis set superposition errors.[30] For all MP2 calculations on monomers and complexes, s and p orbitals below the valence shell were frozen in the Hartree−Fock MOs. These calculations were carried out using the Gaussian 98 program[31] on the Cray SV1 computer at the Ohio Supercomputer Center.

Experimental Results

Before co-deposition experiments were run, blank spectra of each of the reagents used in this study were obtained in separate experiments. The spectra agreed well with published data[4,10,32−34] and spectra previously obtained in this laboratory.[35−37] The D/H ratio in the DCl experiments was approximately 3/1, while the D/H ratio in the D_2O_2 experiments was about 9/1. Bands due to the known complexes[14] of each of the hydrogen halides with H_2O were seen very weakly in these experiments, due to the low level presence of impurity H_2O.

H_2O_2 + HF. Samples of Ar/HF were co-deposited with samples of Ar/H_2O_2 in approximately 20 twin jet experiments. While the concentration of these samples could not be determined accurately due to the methods of preparation, the Ar/HF ratios were estimated to range from 200/1 to 2000/1. The Ar/H_2O_2 ratios were estimated to be in a similar range. In each of these experiments, bands not attributable to either parent were observed at 599 (multiplet), 815 (doublet), 1304, 3603 and 3634 cm^{-1}. The band at 3634 cm^{-1} was particularly intense and relatively sharp, while the band at 3603 cm^{-1} was of medium intensity. The remainder of the product bands were significantly weaker, but nonetheless were reproduced in all of the experiments. It is noteworthy that in all of these experiments, conducted over a wide range of sample concentrations, these product bands appeared to maintain a constant intensity ratio with respect to one another, to the degree that the weaker product bands could be accurately measured. Several of these matrices were subsequently annealed to approximately 30 K, and recooled. All of the product bands grew slightly upon annealing; bands due to HF aggregates and H_2O_2 aggregates were noticed as well.

Several experiments were conducted in which HF was co-deposited with H_2O_2 into nitrogen matrices. In each experiment, a total of 4 product bands were noted, at 443, 669, 3480, and 3648 cm^{-1}; Figure 3 shows the infrared spectrum in the 3300−3700 cm^{-1} region for a typical experiment. The band at 3480 cm^{-1} is by far the most intense of these four bands. When one of these matrices was subsequently annealed to 25 K, the bands at 443, 669, and 3480 cm^{-1} significantly decreased in intensity, while the band at 3648 cm^{-1} was unchanged. In another experiment, at higher HF levels, the same four bands were noted. However, the bands at 443, 669, and 3480 cm^{-1} maintained a constant intensity ratio with respect to one another, while the band at 3648 cm^{-1} grew more rapidly than did the first three. The product bands observed in the HF/ H_2O_2 experiments in argon and nitrogen matrices are listed in Table 1.

An extensive series of experiments was also carried out in which samples of Ar/HF were co-deposited with samples of Ar/D_2O_2. As noted above, the level of isotopic enrichment was approximately 90%, so that bands due to HDO_2 were also seen, including the O−H stretching band at 3585 cm^{-1}. In all of these experiments, product bands were observed at 597 (multiplet), 807 (doublet), 2630, 2643, 3596, and 3630 cm^{-1}. The 3630 cm^{-1} band was clearly the most intense, followed by the 3596 cm^{-1} band. The remaining product bands were much weaker,

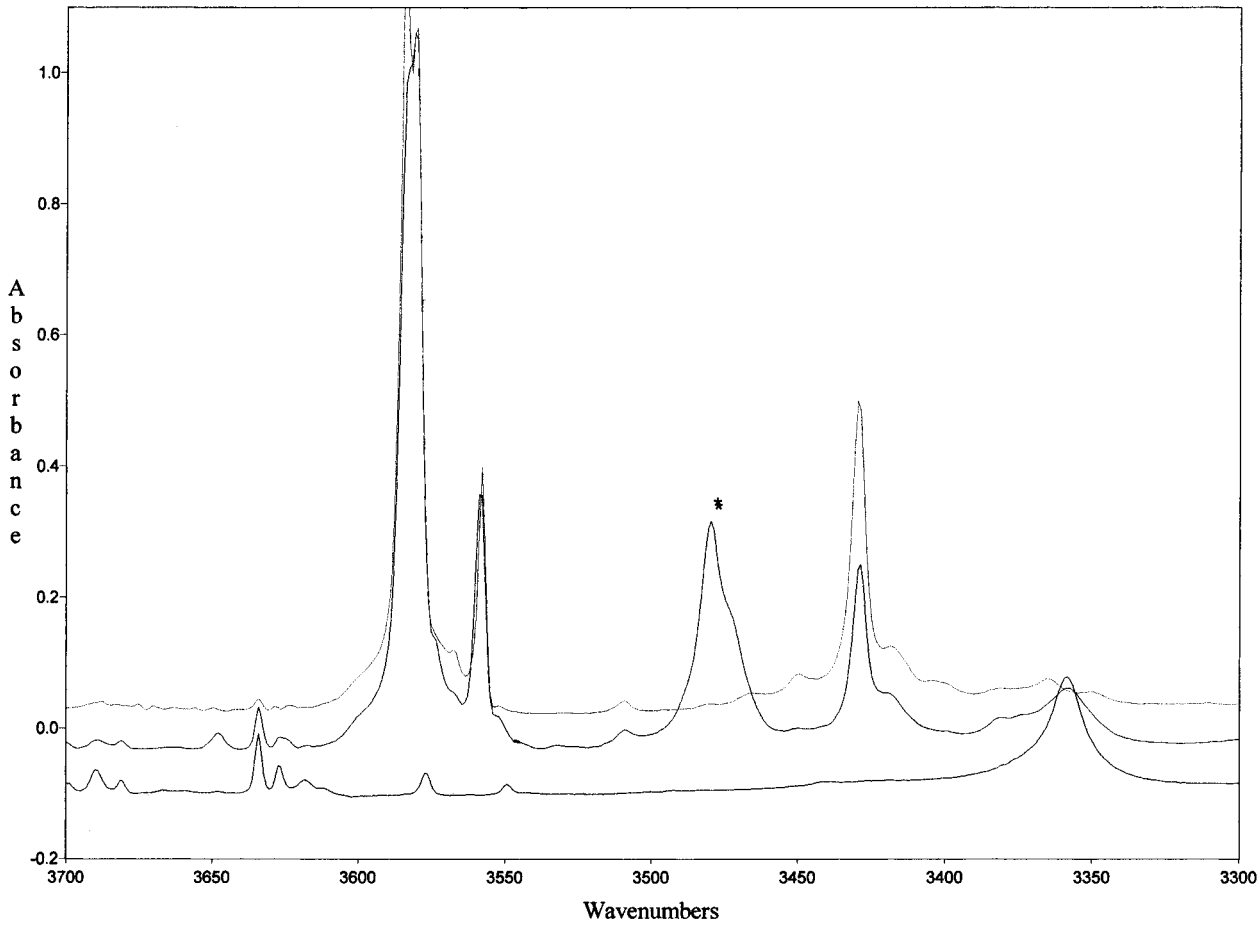

Figure 3. Infrared spectrum between 3300 and 3700 cm^{-1} of a matrix prepared by the co-deposition of a sample of N_2/HF with a sample of N_2/H_2O_2 (middle trace), compared to a sample of N_2/HF (bottom trace) and a sample of N_2/H_2O_2 (top trace). The bands marked with an * are due to product species.

TABLE 1: Band Positions for the 1:1 Complex of H_2O_2 with HF

complex	ν(argon), cm^{-1}	$\nu(N_2)$, cm^{-1}	assignment
FH:H_2O_2	3634	3480	ν_s, HF
	3603		ν_s, OH
	1304		ν_b, OOH
	815[a]		ν_l, HF
	599[a]	669	ν_l, HF
		443	ν_τ, HF
FH:D_2O_2	3630	3482	ν_s, HF
	3596		ν_s, OH
	2643		ν_s, OD
	2630		ν_s, OD
	807[a]	700	ν_l, HF
	597[a]	671	ν_l, HF

[a] - multiplet, see text.

but nonetheless clear and reproducible. Throughout this series of experiments, these product bands maintained a constant intensity ratio with respect to one another. Annealing several of these matrices led to a slight growth in the product bands.

HF and D_2O_2 were also co-deposited into N_2 matrices in several experiments. In the first experiment, four product bands were observed, at 671, 700, 3482, and 3648 cm^{-1}, with the 3482 cm^{-1} band being clearly the most intense of the four. In a second experiment, the HF concentration was increased, and all four bands grew in intensity. The bands at 671, 700 and 3482 cm^{-1} grew at the same rate, while the band at 3648 cm^{-1} grew much more rapidly. When this sample was subsequently annealed, the bands at 671, 700, and 3482 cm^{-1} disappeared, while the band at 3648 cm^{-1} remained with approximately the same intensity.

H_2O_2 + HCl. In an initial experiment, a sample of Ar/H_2O_2 (with the UHP held at 15 °C) was co-deposited with a sample of Ar/HCl = 500/1. Several product bands were noted including a band of medium intensity at 2711 cm^{-1}, several weaker bands near 2694 and 2678 cm^{-1}, and new features at 3563 and 3569 cm^{-1}. Upon annealing this matrix all of the product bands increased in intensity. A total of four additional experiments using argon as the matrix gas were conducted. In all the experiments the product bands were present with intensities proportional to the reactant concentrations. Annealing of the matrices gave similar results to the first experiment.

In a second series of experiments, a sample of N_2/H_2O_2 was co-deposited with a sample of N_2/HCl = 500/1. A very distinct product band was noted at 2654 cm^{-1} with a shoulder at 2644 cm^{-1}. In addition, well resolved new features were observed at 3563 and 3569 cm^{-1}. Upon annealing this matrix, all of the product bands grew by approximately 100%, as illustrated for the band at 2654 cm^{-1} in Figure 4. Four additional experiments using nitrogen as the matrix gas were conducted in which the temperature of the UHP (i.e., the concentration of H_2O_2) was varied from 9 °C to 12 °C and the N_2/HCl concentration varied from 250/1 to 500/1. In all the experiments the band at 2654 cm^{-1} with a shoulder at 2644 cm^{-1} along with the features at 3563 and 3569 cm^{-1} were present with intensities that varied directly with the concentration of the reactants. All of these matrices were annealed, and the product bands significantly

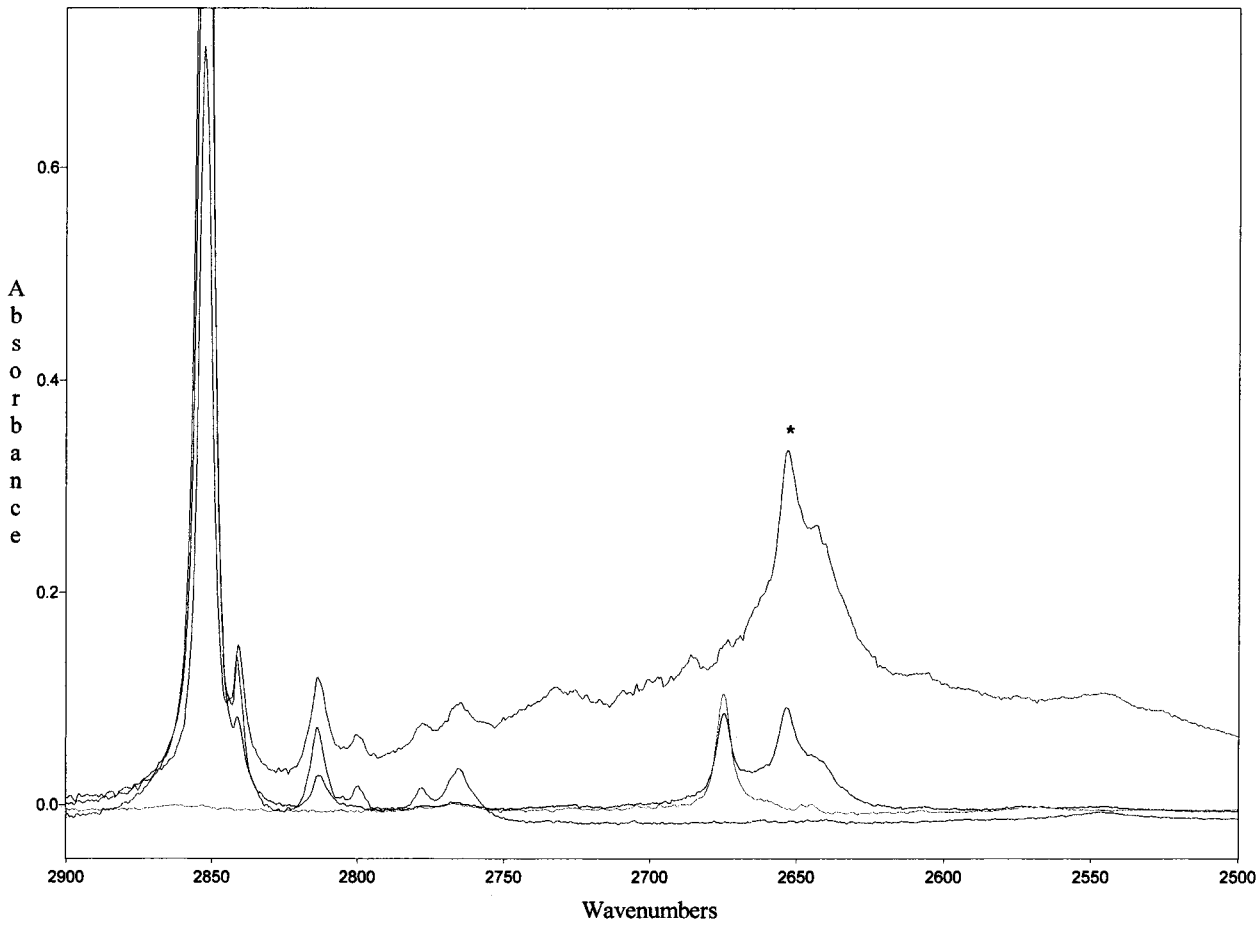

Figure 4. Infrared spectrum, between 2500 and 2900 cm^{-1}, of a matrix prepared by the co-deposition of a sample of $N_2/HCl = 500$ with a sample of N_2/H_2O_2 (second trace from top), compared to the same sample after annealing (top trace), a sample of N_2/H_2O_2 (third trace from top), and a sample of $N_2/HCl = 500$ (bottom trace). The band marked with an * is due to the 1:1 complex.

TABLE 2: Band Positions for the 1:1 Complexes of H_2O_2 with HCl and HBr

complex	ν(argon), cm^{-1}	$\nu(N_2)$, cm^{-1}	assignment
$ClH:H_2O_2$	3569	3569	ν_s, OH
	3563	3563	ν_s, OH
	2711	2654	ν_s, HCl
$ClH:D_2O_2$	2709		ν_s, OD
$ClD:H_2O_2$	1963	1924	ν_s, DCl
$BrH:H_2O_2$	3577	3570	ν_s, OH
	2437	2381	ν_s, HBr
$BrH:D_2O_2$	3580	3571	ν_s, OD
	2639	2635	ν_s, OD
	2435	2381	ν_s, HBr

increased in intensity. The product bands observed for HCl/H_2O_2 in argon and nitrogen matrices are listed in Table 2.

Three experiments were conducted in which HCl and D_2O_2 were co-deposited into nitrogen matrices. Unfortunately, the expected product band (corresponding to the 2654 cm^{-1} band in HCl/H_2O_2) coincided with the O−D stretch of the parent D_2O_2, so that the exact position of the product band(s) could not be determined. Two experiments were also conducted using argon as the matrix gas. In these experiments the UHP was held at 15 °C, with Ar/HCl = 500/1 in the first experiment and 1000/1 in the second. In both experiments, one weak product band was observed at 2709 cm^{-1}, the intensity of which was approximately twice as great in the first experiment compared to the second.

In a related experiment, a sample of N_2/H_2O_2 was co-deposited with a sample of $N_2/DCl = 250/1$. One weak, asymmetric product band was noted at 1924 cm^{-1}. Upon annealing, this product band grew and no new bands were formed. Two additional experiments using nitrogen as the matrix gas were conducted in which the temperature of the UHP (concentration of H_2O_2) was 12 °C and the N_2/DCl concentration varied from 250/1 to 500/1. In both experiments the band at 1924 cm^{-1} was present with an intensity that varied directly with the concentration of the reactants. In the experiment with $N_2/DCl = 250/1$, the matrix was annealed to 31 K. The band at 1924 cm^{-1} increased in intensity in a manner similar to the increase in intensity observed in the corresponding N_2/HCl experiments. Two experiments were also conducted in which DCl and H_2O_2 were co-deposited into argon matrices. In the first, argon swept over UHP at 15 °C was co-deposited with a sample of Ar/DCl = 100/1 and in the second argon swept over UHP at 12 °C was co-deposited with a sample of Ar/DCl = 500/1. In both experiments, a single product band was observed at 1963 cm^{-1}.

H_2O_2 + HBr. These two reagents were co-deposited in a series of experiments into argon matrices. In an initial experiment, with Ar/HBr = 250/1 and the UHP held at 18 °C, a distinct band of medium intensity was observed at 2437 cm^{-1}, along with weak features on the low energy side at 2394, 2406, and 2421 cm^{-1}. In addition, a clear shoulder on the main O−H stretching peak of H_2O_2 was seen at 3577 cm^{-1}. In several additional experiments, the concentration of HBr was varied from 500/1 to 100/1. In each experiment, these same features

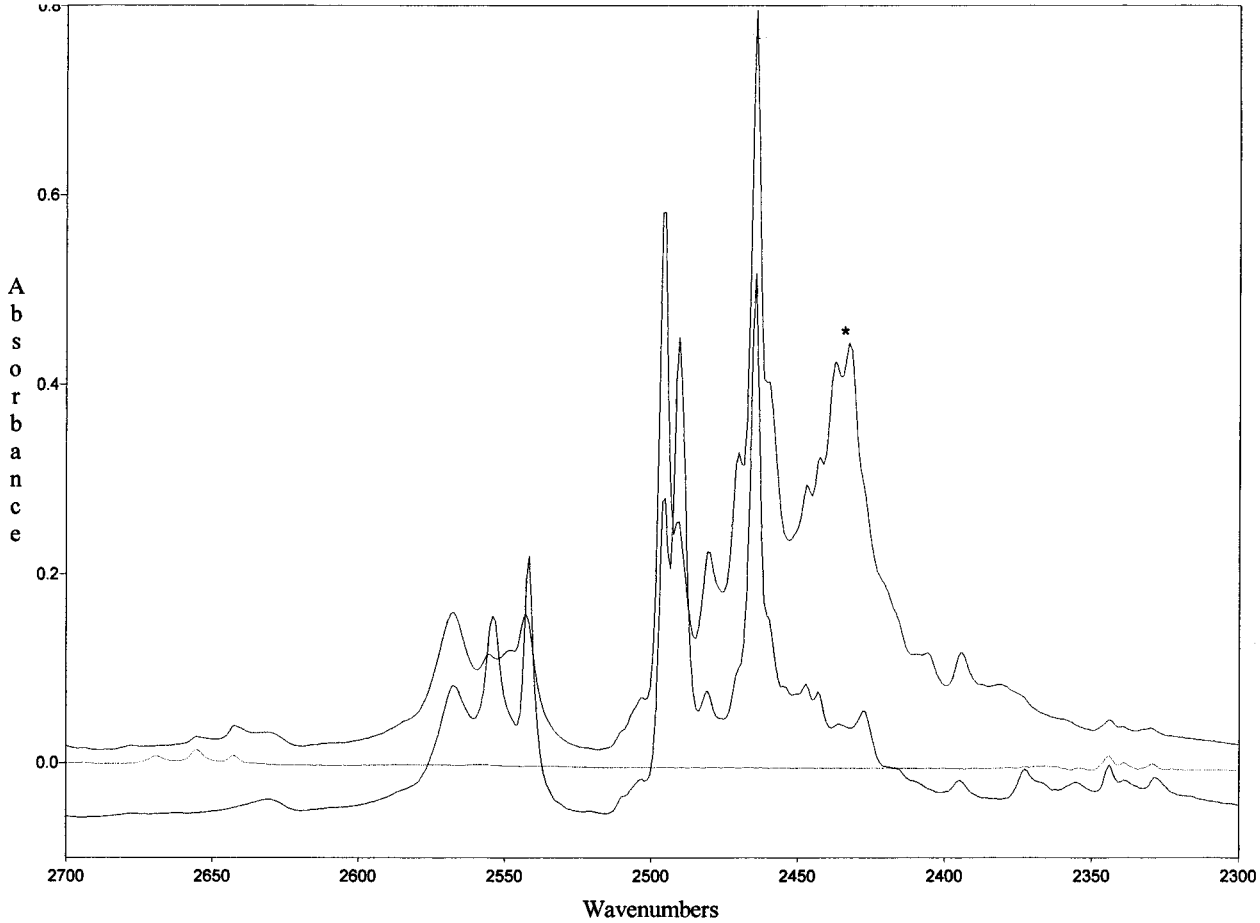

Figure 5. Infrared spectrum, between 2300 and 2700 cm^{-1}, of a sample prepared by the co-deposition of a sample of Ar/HBr = 100 with a sample of Ar/H_2O_2 (top trace), compared to a sample of Ar/H_2O_2 (middle trace), and a sample of Ar/HBr = 100 (bottom trace). The band marked with an * is due to the 1:1 complex.

were observed, with intensities proportional to the concentration of the sample. In the experiment with Ar/HBr = 100/1, the 2437 cm^{-1} was particularly intense and distinct, as shown in Figure 5, and the band at 3577 cm^{-1} was clearly resolved from the H_2O_2 parent band.

A parallel set of experiments was conducted in which H_2O_2 and HBr were co-deposited into N_2 matrices. In each experiment, a moderately intense, somewhat broad absorption was observed at 2381 cm^{-1}. In addition, a distinct absorption was noted at 3570 cm^{-1}, on the low-energy side of the O−H parent stretching modes at 3583 cm^{-1}. No other product bands were observed in the spectrum. In each experiment in this set, these same two features were observed, with intensities proportional to the concentration of the sample. Table 2 summarizes the product bands observed in these experiments.

Experiments were also conducted in which samples of D_2O_2 were co-deposited with HBr into both argon and nitrogen matrices. When argon was employed, a very strong, broad band was observed at 2435 cm^{-1}, with an appearance and position that was very similar to the major band observed in the H_2O_2/HBr/Ar experiments described above. In addition, a weak band was observed at 2639 cm^{-1}, on the low energy side of the O−D stretching bands of D_2O_2 at 2645 cm^{-1}. Last, a weak band was observed at 3580 cm^{-1}, near the O−H stretching mode of HDO_2. When HBr and D_2O_2 were deposited into N_2 matrices, similar results were obtained. An intense, broad band was seen at 2381 cm^{-1}, just as in the H_2O_2/HBr/N_2 experiments, along with weaker but distinct features at 2635 and 3571 cm^{-1}.

Results of ab Initio Calculations. The equilibrium open and cyclic complexes HF:H_2O_2, HCl:H_2O_2, and HBr:H_2O_2 have C_1 symmetry. The open structures are stabilized by essentially linear X−H···O hydrogen bonds, whereas the cyclic structures are stabilized by two distorted, nonlinear X−H···O and O−H···X hydrogen bonds. Table 3 summarizes the important structural parameters for the open and cyclic complexes. Table 4 presents MP2/aug′-cc-pVDZ and MP2/aug′-cc-pVTZ electronic binding energies. Binding enthalpies at 0 K based on these electronic energies and MP2/aug′-cc-pVDZ zero-point vibrational energies are also reported for these complexes and their deuterated isotopomers in Table 4. All complexes with open structures and the cyclic HOOH:FH complex have MP2/aug′-cc-pVDZ binding energies that are greater than the MP2/aug′-cc-pVTZ energies, although the differences are small. The binding energies of open and cyclic HCl:H_2O_2 isomers computed with these two basis sets are identical, whereas the MP2/aug′-cc-pVDZ binding energy of HOOH:BrH is slightly less than the MP2/aug′-cc-pVTZ energy. However, the binding energies for corresponding structures computed with these two basis sets differ by no more than 0.3 kcal/mol. MP2/aug′-cc-pVTZ electronic binding energies, and binding enthalpies based on these energies and MP2/aug′-cc-pVDZ zero point vibrational energies will be discussed below.

HF:H_2O_2. Of the complexes formed between the hydrogen halides and H_2O_2, those with HF are the most strongly bound. The MP2/aug′-cc-pVTZ electronic binding energies are −7.2 and −7.5 kcal/mol for the open and cyclic structures, respec-

TABLE 3: Calculated Hydrogen-Bonded O−X and O−H Distances (R_e, Å), and H−X−O and H−O−X Angles (°) for Open and Cyclic Complexes of the Hydrogen Halides (HX) with H_2O_2

X−H···O Hydrogen bond				
open	R_e(X−O)	R_e(X−H)[a]	<H−X−O	μ (D)
FH:O_2H_2	2.703	0.938	3.0	4.35
ClH:O_2H_2	3.226	1.301	0.4	3.83
BrH:O_2H_2	3.415	1.432	0.3	3.61
X−H···O Hydrogen Bond				
cyclic	R_e(X−O)	R_e(X−H)[a]	<H−X−O	μ (D)
HOOH:FH	2.602	0.943	18.8	2.03
HOOH:ClH	3.112	1.306	15.3	1.70
HOOH:BrH	3.293	1.436	15.9	1.57
O−H···X Hydrogen Bond				
cyclic	R_e(O−X)	R_e(O−H)[a]	<H−O−X	
HOOH:FH	2.902	0.977	36.4	
HOOH:ClH	3.420	0.976	34.6	
HOOH:BrH	3.573	0.976	32.9	

[a] Monomer distances: HF = 0.924 Å; HCl = 1.288 Å; HBr = 1.420 Å; H_2O_2 = 0.972 Å.

TABLE 4: MP2/aug′-cc-pVDZ and MP2/aug′-cc-pVTZ Binding Energies (ΔE_e, kcal/mol) and Binding Enthalpies ($\Delta H°$, kcal/mol) for HX:H_2O_2 and their Deuterated Analogues[a]

Open Complexes				
	FH:O_2H_2	FH:O_2D_2	FD:O_2H_2	FD:O_2D_2
ΔE_e	−7.4(−7.2)	−7.4(−7.2)	−7.4(−7.2)	−7.4(−7.2)
ΔH^0	−5.1(−4.9)	−5.3(−5.1)	−5.5(−5.3)	−5.6(−5.4)
	ClH:O_2H_2	ClH:O_2D_2	ClD:O_2H_2	ClD:O_2D_2
ΔE_e	−5.2(−4.9)	−5.2(−4.9)	−5.2(−4.9)	−5.2(−4.9)
ΔH^0	−3.5(−3.2)	−3.6(−3.3)	−3.8(−3.5)	−3.9(−3.6)
	BrH:O_2H_2	BrH:O_2D_2	BrD:O_2H_2	BrD:O_2D_2
ΔE_e	−4.7(−4.6)	−4.7(−4.6)	−4.7(−4.6)	−4.7(−4.6)
ΔH^0	−3.3(−3.2)	−3.3(−3.2)	−3.5(−3.4)	−3.6(−3.5)
Cyclic Complexes				
	HOOH:FH	DOOD:FH	HOOH:FD	DOOD:FD
ΔE_e	−7.7(−7.5)	−7.7(−7.5)	−7.7(−7.5)	−7.7(−7.5)
ΔH^0	−5.1(−4.9)	−5.3(−5.1)	−5.4(−5.2)	−5.6(−5.4)
	HOOH:ClH	DOOD:ClH	HOOH:ClD	DOOD:ClD
ΔE_e	−5.1(−5.1)	−5.1(−5.1)	−5.1(−5.1)	−5.1(−5.1)
ΔH^0	−3.2(−3.2)	−3.4(−3.4)	−3.6(−3.6)	−3.7(−3.7)
	HOOH:BrH	DOOD:BrH	HOOH:BrD	DOOD:BrD
ΔE_e	−4.6(−4.9)	−4.6(−4.9)	−4.6(−4.9)	−4.6(−4.9)
ΔH^0	−3.0(−3.3)	−3.1(−3.4)	−3.3(−3.6)	−3.4(−3.7)

[a] MP2/aug′-cc-pVDZ electronic energies; MP2/aug′-cc-pVTZ energies in parentheses.

tively. However, the binding enthalpies at 0 K for these two isomers are identical at −4.9 kcal/mol. As expected, isotopic substitution of D for H in either HF or H_2O_2 increases the stabilities of both open and cyclic structures by 0.2 to 0.5 kcal/mol. However, the binding enthalpies of the open and cyclic forms of corresponding isotopomers are essentially identical. This suggests that the experimental IR spectrum obtained for the HF:H_2O_2 system could be a combination of two spectra arising from the two isomers. However, due to the apparent flatness of the potential surface in the region connecting these structures, only one isomer may be present. This will be discussed further when the experimental spectra are analyzed below.

As evident from Table 3, the open FH:O_2H_2 structure is stabilized by an essentially linear F−H···O hydrogen bond, with an H−F−O angle of only 3.0°. The intermolecular F−O distance is 2.703 Å and the F−H distance is 0.938 Å, which is 0.014 Å longer than the monomer F−H distance. With the exception of the intermolecular distance, the structure of the open FH:O_2H_2 isomer is similar to that of open ClH:O_2H_2 illustrated in Figure 1.

Similarly, except for intermolecular distances, cyclic HOOH:FH is structurally similar to cyclic HOOH:ClH illustrated in Figure 2. The HOOH:FH complex is stabilized by two distorted F−H···O and O−H···F hydrogen bonds. In the O−H···F hydrogen bond the O−F distance is 2.902 Å and the O−H distance is 0.977 Å, only slightly longer than the O−H distance in H_2O_2. The H−O−F angle is 36.4°. These structural parameters are indicative of a weak, nonlinear hydrogen bond. The F−H···O hydrogen bond is also nonlinear, but with an H−F−O angle of 18.8°, this hydrogen bond is not as distorted as the O−H···F bond. The F−O distance is 2.602 Å, which is shorter than the F−O distance in the open complex. Moreover, the F−H distance is 0.943 Å, longer than the F−H distance in the open structure. The shorter F−O and the longer F−H distances are surprising, since the open structure with a single, essentially linear hydrogen bond would be expected to have the shorter F−O distance and the longer F−H distance. On the basis of these structural parameters, it would be expected that the F−H stretch should have a lower frequency in the cyclic isomer compared to the open one. Three strong bands are associated with F−H and O−H stretching vibrations in the computed spectra of both isomers, due to accidental coupling between F−H and O−H stretches, and these three occur at lower frequencies in the cyclic isomer. The vibrational spectra of both isomers will be discussed below.

HCl:H_2O_2. HCl is a weaker donor for hydrogen bond formation, with the result that the MP2/aug′-cc-pVTZ electronic binding energies of the open and cyclic HCl:H_2O_2 complexes are 2.3 and 2.4 kcal/mol less than those of the corresponding HF:H_2O_2 complexes. The binding enthalpies of the open and cyclic isomers of HCl:H_2O_2 are identical at −3.2 kcal/mol. Isotopic substitution of D for H in either HCl or H_2O_2 slightly increases binding enthalpies. However, the binding enthalpies of corresponding open and cyclic isotopomers differ by no more than 0.1 kcal/mol.

The open isomer ClH:O_2H_2 that is shown in Figure 1 is stabilized by a linear Cl−H···O hydrogen bond. The intermolecular distance is 3.226 Å, and the Cl−H distance is 1.301 Å. This distance is slightly longer than the monomer H−Cl distance of 1.288 Å. The cyclic HOOH:ClH complex, shown in Figure 2, is stabilized by two distorted hydrogen bonds, and except for the intermolecular distances, is structurally similar to the HOOH:FH complex. In this and the other cyclic isomers, the hydrogen-bonded X, O, and H atoms are very nearly coplanar. The hydrogen bond O−Cl distance in the O−H···Cl hydrogen bond is 3.420 Å and the O−H distance is 0.976 Å. This hydrogen bond is very nonlinear, with an H−O−Cl angle of 34.6°. The Cl−H···O hydrogen bond in the cyclic structure is also nonlinear, with an H−Cl−O angle of 15.3°. The Cl−O distance is again shorter and the Cl−H distance longer in the cyclic structure relative to the open, and the cyclic isomer again has the lower-frequency Cl−H stretching band.

HBr:H_2O_2. Among the complexes of the hydrogen halides with hydrogen peroxide, those containing HBr have the lowest

electronic binding energies. The MP2/aug′-cc-pVTZ binding energies of the open and cyclic isomers are similar at −4.6 and −4.9 kcal/mol, respectively, while the binding enthalpies are −3.2 and −3.3 kcal/mol, respectively. Isotopic substitution of D for H increases binding enthalpies by 0.1 to 0.4 kcal/mol. The binding enthalpies of corresponding open and cyclic isotopomers differ by no more than 0.2 kcal/mol, and are very similar to the binding enthalpies of the corresponding ClH:H_2O_2 complexes.

Except for the intermolecular distances, the open and cyclic complexes are structurally similar to the open and cyclic complexes of HF:H_2O_2 and HCl:H_2O_2. The open isomer is stabilized by a linear Br−H···O hydrogen bond, with Br−O and Br−H distances of 3.415 and 1.432 Å, respectively. The Br−H distance is slightly elongated relative to the monomer distance of 1.420 Å. The cyclic isomer is stabilized by two distorted, nonlinear Br−H···O and O−H···Br hydrogen bonds. The H−Br−O and H−O−Br angles are 15.9 and 32.9°, respectively. In the Br−H···O hydrogen bond, the Br−O distance of 3.293 Å is shorter and the Br−H distance of 1.436 Å is slightly longer than the Br−O and Br−H distances in the open isomer. In the O−H···Br hydrogen bond, the O−Br and O−H distances are 3.573 and 0.976 Å, respectively.

Discussion

Several common features were observed in the experimental spectra recorded when H_2O_2 was co-deposited with HF, HCl, and HBr in Ar and N_2 matrices. These general features will be discussed first, followed by discussion and assignments of spectral bands for each system.

The growth of strong new bands upon co-deposition of HF, HCl, and HBr with H_2O_2 into cryogenic matrices demonstrates the presence of one or more new species in these experiments. Most apparent was the growth of a quite intense product band for each system, observed 100−400 cm^{-1} to the red of the monomer HX stretching band, as well as one or two weaker bands very near the O−H stretching bands of the H_2O_2 monomer. These product bands were seen in all experiments with a given pair of reactants. Moreover, all of the product bands maintained a constant intensity ratio with respect to one another throughout the set of experiments for each system, except for the 3648 cm^{-1} band for the HF/H_2O_2/N_2 system. This band was relatively more intense than the other product bands at higher sample concentrations. In addition, when these matrices were annealed, the 3648 cm^{-1} band showed quite different behavior from the other product bands, requiring that it be assigned to a different absorber. All of these observations strongly suggest that *a single product species is formed for each system*, except for the HF/H_2O_2/N_2 system. For this system, the bands at 443, 669, and 3480 cm^{-1} can be assigned to one product while the 3648 cm^{-1} band must be assigned to a different product.

With the exception of the bands near 600 and 800 cm^{-1} for the HF/H_2O_2 system, all other bands lie near bands observed for either H_2O_2 or the hydrogen halide. This suggests that a weakly bound complex is formed in which the two monomers are perturbed but maintain their structural integrity. As noted above, the most intense band was observed 100−400 cm^{-1} to, the red of the H−X parent stretching mode. This band for each system *did not shift* significantly when D_2O_2 was substituted for H_2O_2, but *shifted dramatically* when DCl was substituted for HCl ($\nu_H/\nu_D = 1.38$). The large shift of the H−X stretching band is consistent with, and strongly supports formation of a hydrogen-bonded complex between H_2O_2 and each of the hydrogen halides.[38] This is also consistent with many earlier studies of hydrogen-bonded complexes of the hydrogen halides in inert matrices.[14−16]

The experimental data strongly suggest that the single product formed in each experiment is a 1:1 hydrogen-bonded complex of H_2O_2 with each hydrogen halide. The fact that the product bands are observed at quite low concentrations argues against the single product being a higher complex with 2:1 or 1:2 XH:H_2O_2 stoichiometry. Moreover, it would be difficult to envision formation of a higher complex without initial formation of the 1:1 complex, yet only a single product was observed for all systems, except the HF/H_2O_2/N_2 system. For this system, the 3648 cm^{-1} band must be assigned to a different absorber. On the basis of the concentration dependence and annealing behavior of this band, assignment to a complex of higher stoichiometry is appropriate. However, the observation of a single band for this absorber precludes determination of the precise stoichiometry of this second complex, although the fact that it appeared at higher HF concentrations suggests that it might be a 2:1 HF:H_2O_2 complex. The conclusion that the primary product for the HF/H_2O_2 system and only product for the HCl/H_2O_2 and HBr/H_2O_2 systems is the 1:1 complex is also supported by the MP2/aug′-cc-pVDZ calculations. In fact, the calculations suggest that two different 1:1 complexes, one open and one cyclic, are stable. The isomer that is more likely to be present in the matrix will be identified below, based on comparisons between experimental and computed band shifts.

HF + H_2O_2. The most intense band in the IR spectrum, at 3634 cm^{-1} in solid argon and at 3480 cm^{-1} in solid N_2, is significantly red-shifted from the parent H−F stretching band, and is best assigned to the H−F stretching mode in the 1:1 complex. The small 4 cm^{-1} shift of this band when D_2O_2 was substituted for H_2O_2 further supports assignment to the H−F stretch. As noted previously, the calculated spectra predict three strong bands for both cyclic and open isomers due to accidental coupling between the F−H and the two O−H stretching vibrations. For the open isomer, the computed shift of one of these bands is in good agreement with the experimental shift of the H−F stretching band, as evident from Table 2. The computed shift of the second band is small relative to the O−H stretching band in H_2O_2, and corresponds to the product band at 3603 cm^{-1}. The computed shift of the second O−H stretching mode is only 1 cm^{-1}, and cannot be resolved from the intense parent peak of H_2O_2. In contrast, the computed shifts of the three strong bands in the cyclic isomer are much larger, as shown in Table 5. If the cyclic isomer were present in the matrix, three shifted intense bands should have been observed in the experimental spectra, as shown by the intensities given in Table 5.

Several additional product bands were observed in the experimental spectra, including a weak band at 1304 cm^{-1}, at higher frequency relative to the parent H_2O_2 bending mode near 1277 cm^{-1}. This band disappeared when D_2O_2 was substituted for H_2O_2, indicating that it must be associated with the H_2O_2 subunit in the complex (The corresponding band in the D_2O_2 complex band was not detected due to lower intensities for the deuterated species). The H_2O_2 antisymmetric bending mode is calculated to shift slightly. The proximity of this product band to the parent mode supports assignment of this band to the antisymmetric bending mode of H_2O_2 in the 1:1 complex between H_2O_2 and HF. In addition, the product band at 443 cm^{-1} in N_2 also disappeared when D_2O_2 was substituted for H_2O_2. This band lies at a higher frequency than the parent H_2O_2 torsional mode which has been observed[39] by other researchers at 373 cm^{-1} in solid argon. (The monomer band lies below the

TABLE 5: Calculated and Experimental Band Shifts for the H−X and O−H Stretching Modes of the 1:1 Complexes

	$\Delta\nu_{HX}$(calc, open)	*I*(calc)	$\Delta\nu_{HX}$(calc, cyclic)	*I*(calc.	$\Delta\nu_{HX}$(expt, Ar)	$\Delta\nu_{HX}$(expt, N_2)
HF	−342 cm^{-1}	503	−434 cm^{-1}	281	−316 cm^{-1}	−410 cm^{-1}
HCl	−188	599	−255	526	−162	−204
HBr	−139	435	−194	373	−118	−163
	$\Delta\nu_{OH}$(calc, open)	*I*(calc)	$\Delta\nu_{OH}$(calc, cyclic)	*I*(calc)	$\Delta\nu_{OH}$(expt, Ar)	$\Delta\nu_{OH}$(expt, N_2)
HF	−1,−9 cm^{-1}	145, 335	−16,−59 cm^{-1}	49, 467	+14 cm^{-1}	
HCl	−9,−16	59, 62	−21,−71	65, 85	−14,−20	−13,−19
HBr	−8,−16	60, 61	−21,−71	64, 87	−8	−13

spectral limit of the instrument employed in this study). The calculations predict a +28 cm^{-1} shift for this mode in the open structure, and this band is tentatively assigned to the torsional mode of H_2O_2 in the 1:1 complex with HF.

Multiplets at 599 and 815 cm^{-1} in argon, and a band at 669 cm^{-1} in N_2 were also observed for the FH:H_2O_2 system. These bands shifted only slightly when D_2O_2 was substituted for H_2O_2, appearing at 597 and 807 cm^{-1} in argon, and at 671 and 700 cm^{-1} in N_2. Neither H_2O_2 nor the hydrogen halide has vibrational modes near these bands, so assignment to a perturbed mode of either monomer is *not* appropriate. However, the formation of a 1:1 complex between a linear molecule and a nonlinear molecule results in the loss of 3 translational and 2 rotational degrees of freedom, and the creation of 5 new intermolecular vibrational modes which typically lie at quite low frequencies. Two of these modes, the librational modes, have been observed[15,16] in the spectral region between 500 and 1000 cm^{-1} in a number of hydrogen-bonded complexes of HF. For the FH:H_2O complex, these modes were observed as quartets, centered at 622 and 734 cm^{-1}, with the quartet structure attributed to inversion doubling.[40] For the H_2O_2 complex with HF, these modes are calculated to occur at 678 and 744 cm^{-1} (open structure) and at 747 and 831 cm^{-1} (cyclic structure), with small deuterium shifts (−3 and −21 cm^{-1} for the open structure, and −34 and −15 cm^{-1} for the cyclic structure). The computed frequencies for these bands agree reasonably well with the experimental frequencies, although the deuterium shifts for the open structure are in better agreement with the experimental shifts. Thus, assignment to these two bands to librational modes is made. The splittings observed may be due to inversion doubling, as in the FH:H_2O complex. However, the experimental data obtained in this study are not sufficiently sharp or definitive to support a firm conclusion on this point. It is not clear where the second librational mode of the complex in solid N_2 is located, and whether the lack of observation of this mode is due to low intensity. In any event, the results in the low energy region point out the significant role of the host matrix on low-frequency vibrations.

HCl + H_2O_2. For this pair of reagents, the most intense band in the experimental spectra occurred at 2711 cm^{-1} in argon matrices and at 2654 cm^{-1} in N_2 matrices. These bands shifted significantly to 1963 and 1924 cm^{-1}, respectively, when DCl was substituted for HCl, but did not shifted when D_2O_2 was substituted for H_2O_2. These observations strongly support assignment to the H−Cl stretching mode, red shifted from the parent HCl. The magnitude of the shift in Ar is in good agreement with the computed shift for the open isomer. The product bands at 3563 and 3569 cm^{-1} in both argon and N_2 lie very close to the parent O−H stretching modes of H_2O_2. In addition, these band shifted strongly when D_2O_2 was substituted for H_2O_2. Consequently, they are readily assigned to the two perturbed O−H stretching modes in the 1:1 complex.

HBr + H_2O_2. Two product bands were observed upon the deposition of this pair of reagents, the more intense of which was a band to the red of the parent H−Br stretching mode, at 2437 cm^{-1} in argon and 2381 cm^{-1} in N_2. This band did not shift when D_2O_2 was substituted for H_2O_2, indicating that it must be assigned to the stretching mode of the HBr subunit in the 1:1 complex. As shown in Table 5, the observed shift is in good agreement with the calculated shift for the open isomer. The second band was observed at 3577 cm^{-1} in argon and at 3570 cm^{-1} in N_2, on the low energy side of the O−H stretching modes of parent H_2O_2. These bands shifted to 2639 and 2635 cm^{-1} in argon and N_2, respectively, when D_2O_2 was substituted for H_2O_2. Thus, they are readily assigned to an O−H stretching mode of the H_2O_2 subunit in the 1:1 complex.

Structure of the 1:1 Complex. As noted above, the experimental spectra, particularly in the H−X stretching region, strongly support the formation of a single 1:1 complex, despite the fact that the calculations predict two complexes with similar binding energies. While the experimental spectra alone cannot distinguish between the two isomers, comparison of computed and experimental frequency shifts suggests that it is the open isomer which is present in the matrix. As evident from Table 5, the computed shifts of the X−H stretching band in the 1:1 complexes with open structures agree with the experimental band shifts in Ar, overestimating these by 26, 26, and 21 cm^{-1} in FH:O_2H_2, ClH:O_2H_2, and BrH:O_2H_2, respectively. The computed shifts for the cyclic isomers overestimate the experimental shifts in Ar by about 100 cm^{-1}, and are even larger than the experimental shifts observed in N_2. Since the interaction between the complex and the matrix is weaker in Ar than in N_2, and since the computed spectra refer specifically to the gas phase, the computed band shifts should be closer to those observed experimentally in Ar. Moreover, it is also apparent from Table 5 that the computed shifts of the O−H stretching bands in the complexes are smaller in the open structures compared to the cyclic ones, and that the shifts for the open isomers are in better agreement with the experimental shifts. These comparisons support the suggestion that it is the open isomers that give rise to the experimentally observed spectra.

Further Considerations

The role of the matrix is apparent from the results presented here. The matrix not only influences the frequency shifts of the different vibrational modes of these complexes, but also determines which of the two nearly isoenergetic isomers is present in the matrix. It appears that the matrix preferentially stabilizes the open form of the complex, which is calculated to have a dipole moment that is more than twice as large as the dipole moment of the cyclic form, as shown in Table 3. The larger dipole moment leads to a stronger interaction between the complex and the matrix material, whereby the complex polarizes the adjacent matrix atoms or molecules, and these in turn, further polarize the complex. It would be of considerable interest to determine whether both isomers of these complexes could be observed in the gas phase. Microwave spectroscopy

in supersonic expansions might provide the best opportunity to resolve this question.

Finally, it is informative to compare matrix effects on the IR spectra of complexes of the hydrogen halides with H_2O_2 as the base to those with NH_3. In the present study, it was observed that the computed harmonic gas-phase shifts of the X−H stretching bands in the open isomers are in good agreement with the shifts observed experimentally in an Ar matrix. This implies that the anharmonicity corrections in the complexes are not significantly different from those in the corresponding HX monomers. Moreover, the experimental data indicate that changing the matrix material from Ar to N_2 results in relatively small changes in X−H stretching frequencies, decreasing these by 154, 57, and 56 cm^{-1} in $FH:O_2H_2$, $ClH:O_2H_2$, and $BrH:O_2H_2$, respectively.

The behavior of the hydrogen halide complexes with NH_3 is quite different. While the computed shift of the harmonic F−H stretching band in $FH:NH_3$ is in reasonable agreement with that observed experimentally in an Ar matrix, the harmonic approximation fails to reproduce these shifts for $ClH:NH_3$ and $BrH:NH_3$.[25,41] The computed harmonic frequency shifts underestimate the experimental shifts in these complexes by 750 and 1100 cm^{-1}, respectively. Moreover, changing the matrix material from Ar to N_2 has very different effects on the experimental proton-stretching frequencies, decreasing this frequency by about 650 cm^{-1} for the $ClH:NH_3$ complex, but increasing it by about the same amount for $BrH:NH_3$.[42] There are a number of related factors, all reflecting the increased proton-accepting ability of NH_3, that are responsible for these differences. These include the much greater strengths of the hydrogen bonds, the increased X−H distances and decreased intermolecular distances, and the larger dipole moments of the complexes with NH_3 compared to those with H_2O_2. Because of the greater proton-accepting ability of NH_3, proton transfer can occur more easily in these complexes, with the result that changing the matrix material can change the type of hydrogen bond present. It has been suggested that the hydrogen bond in $ClH:NH_3$ is a traditional hydrogen-bond in an Ar matrix but a proton-shared hydrogen bond in N_2. By contrast, the hydrogen bond in $BrH:NH_3$ is a proton-shared hydrogen bond in Ar but approaches an ion-pair hydrogen bond in N_2.[25,41] Detailed discussions of anharmonicity and environmental effects on proton-stretching frequencies in hydrogen halide complexes with NH_3 can be found in refs 25 and 41.

Acknowledgment. The National Science Foundation is gratefully acknowledged for support of this research through Grant CHE 9877076.

References and Notes

(1) Gregoire, P. J.; Chaumerliac, N.; Nickerson, E. C. *J. Atmos. Chem.* **1994**, *18*, 247.
(2) Sakugawa, H.; Kaplan, I. R. In *Gaseous Pollutants*; Nriagu, J. O., Ed.; John Wiley and Sons: New York, 1992; Vol. 24.
(3) *Oxidative Stress, Cell Activation and Viral Infection*; Pasquier, C., Ed.; Birkhauser Verlag: Basel, Boston, 1994; p 358.
(4) Petterson, M.; Tuominen, S.; Rasanen, M. *J. Phys. Chem.* **1997**, *101*, 1166.
(5) Lundell, J.; Jolkkonen, S.; Khriachtchev, L.; Pettersson, M.; Rasanen, M. *Chem.—Eur. J.* **2001**, *7*, 1670.
(6) Engdahl, A.; Nelander, B. *Phys. Chem. Chem. Phys.* **2000**, *2*, 3967.
(7) Cradock, S.; Hinchcliffe, A. *Matrix Isolation*; Cambridge University Press: Cambridge, 1975.
(8) Whittle, E.; Dows, D. A.; Pimentel, G. C. *J. Chem. Phys.* **1954**, *22*, 1943.
(9) *Chemistry and Physics of Matrix Isolated Species*; Andrews, L., Moskovitz, M., Eds.; Elsevier Science Publishers: Amsterdam, 1989.
(10) Goebel, J. R.; Ault, B. S.; Del Bene, J. E. *J. Phys. Chem. A* **2001**, *105*, 6430.
(11) Goebel, J.; Ault, B. S.; Del Bene, J. E. *J. Phys. Chem. A* **2000**, *104*, 2033.
(12) Goebel, J.; Ault, B. S.; Del Bene, J. E. *J. Phys. Chem. A* **2001**, *105*, 11365.
(13) Ault, B. S.; Pimentel, G. C. *J. Phys. Chem*. **1973**, *77*, 57.
(14) Andrews, L. *J. Mol. Struct*. **1983**, *100*, 281.
(15) Barnes, A. J. *J. Mol. Struc*. **1983**, *100*, 259.
(16) Andrews, L. *Faraday Discuss. Chem. Soc*. **1988**, *86*, 37.
(17) Ault, B. S. *J. Am. Chem. Soc.* **1978**, *100*, 2426.
(18) Bartlett, R. J.; Silver, D. M. *J. Chem. Phys*. **1975**, *62*, 3258.
(19) Bartlett, R. J.; Purvis, G. D. *Int. J. Quantum Chem.* **1978**, *14*, 561.
(20) Pople, J. A.; Binkley, J. S.; Seeger, R. *Int. J. Quantum Chem. Quantum Chem. Symp*. **1976**, *10*, 1.
(21) Krishnan, R.; Pople, J. A. *Int. J. Quantum Chem*. **1978**, *14*, 91.
(22) Dunning, T. H., Jr. *J. Chem. Phys.* **1989**, *90*, 1007.
(23) Kendall, R. A.; Dunning, T. H., Jr.; Harrison, R. J. *J. Chem. Phys*. **1992**, *96*, 1358.
(24) Woon, D. E.; Dunning, T. H., Jr. *J. Chem. Phys.* **1993**, *98*, 1358.
(25) Del Bene, J. E.; Jordan, M. J. T. *J. Phys. Chem.* **1998**, *108*, 3205.
(26) Hehre, W. J.; Ditchfield, R.; Pople, J. A. *J. Chem. Phys*. **1972**, *56*, 2257.
(27) Hariharan, P. C.; Pople, J. A. *Theor. Chim. Acta* **1973**, *28*, 213.
(28) Spitznagel, G. W.; Clark, T.; Chandrasekhar, J.; Schleyer, P. v. R. *J. Comput. Chem*. **1982**, *3*, 363.
(29) Clark, T.; Chandrasekhar, J.; Spitznagel, G. W.; Schleyer, P. v. R., *J. Comput. Chem*. **1983**, *4*, 294.
(30) Dunning, T. H., Jr. *J. Phys. Chem. A* **2000**, *104*, 9062.
(31) Frisch, M. J.; Trucks, G. W.; Schlegel, H. B.; Scuseria, G. E.; Robb, M. A.; Cheeseman, J. R.; Zakrzewski, V. G.; Montgomery, J. A., Jr.; Stratmann, R. E.; Burant, J. C.; Dapprich, S.; Millam, J. M.; Daniels, A. D.; Kudin, K. N.; Strain, M. C.; Farkas, O.; Tomasi, J.; Barone, V.; Cossi, M.; Cammi, R.; Mennucci, B.; Pomelli, C.; Adamo, C.; Clifford, S.; Ochterski, J.; Petersson, G. A.; Ayala, P. Y.; Cui, Q.; Morokuma, K.; Malick, D. K.; Rabuck, A. D.; Raghavachari, K.; Foresman, J. B.; Cioslowski, J.; Ortiz, J. V.; Baboul, A. G.; Stefanov, B. B.; Liu, G.; Liashenko, A.; Piskorz, P.; Komaromi, I.; Gomperts, R.; Martin, R. L.; Fox, D. J.; Keith, T.; Al-Laham, M. A.; Peng, C. Y.; Nanayakkara, A.; Gonzalez, M.; Challacombe, M.; Gill, P. M. W.; Johnson, B.; Chen, W.; Wong, M. W.; Andres, J. L.; Gonzalez, C.; Head-Gordon, M.; Replogle, E. S.; Pople, J. A. *Gaussian 98*; Gaussian, Inc.: Pittsburgh, PA, 1998.
(32) Maillard, D.; Schriver, A.; Perchard, J. P.; Girardet, C. *J. Chem. Phys.* **1979**, *71*, 505.
(33) Andrews, L.; Johnson, G. L. *Chem. Phys. Lett.* **1983**, *96*, 133.
(34) Barnes, A. J.; Hallam, H. E.; Scrimshaw, G. F. *Trans. Faraday Soc.* **1969**, *65*, 3172.
(35) Ault, B. S. *J. Mol. Struct*. **2000**, *526*, 97.
(36) Bach, S. B. H.; Ault, B. S. *J. Phys. Chem.* **1984**, *88*, 3600.
(37) Ault, B. S. *J. Phys. Chem*. **1979**, *83*, 837.
(38) Pimentel, G. C.; McClellan, A. L. *The Hydrogen Bond*; W. H. Freeman: San Francisco, 1960.
(39) Lannon, J. A.; Verderame, F. D.; Anderson, R. W., Jr. *J. Chem. Phys.* **1971**, *54*, 2212.
(40) Andrews, L.; Johnson, G. L. *J. Chem. Phys*. **1983**, *79*, 3670.
(41) Jordan, M. J. T.; Del Bene, J. E. *J. Am. Chem. Soc*. **2000**, *122*, 2101.
(42) Barnes, A. J.; Wright, M. P. *J. Chem. Soc., Faraday Trans. 2* **1986**, *82*, 153.